

Inverse participation ratio and localization in topological insulator phase transitions

M. Calixto

Departamento de Matemática Aplicada and Instituto Carlos I de Física Teórica y Computacional,
Universidad de Granada,
Fuentenueva s/n, 18071 Granada, Spain
calixto@ugr.es

E. Romera

Departamento de Física Atómica,
Molecular y Nuclear and Instituto Carlos I de Física Teórica y Computacional,
Universidad de Granada,
Fuentenueva s/n, 18071 Granada, Spain
eromera@ugr.es

Fluctuations of Hamiltonian eigenfunctions, measured by the inverse participation ratio (IPR), turn out to characterize topological-band insulator transitions occurring in 2D Dirac materials like silicene, which is isostructural with graphene but with a strong spin-orbit interaction. Using monotonic properties of the IPR, as a function of a perpendicular electric field (which provides a tunable band gap), we define topological-like quantum numbers that take different values in the topological-insulator and band-insulator phases.

PACS numbers: 03.65.Vf, 03.65.Pm, 89.70.Cf,

I. INTRODUCTION

In the last years, the concepts of insulator and metal have been revised and a new category called “topological insulators” has emerged. In these materials, the energy gap Δ between the occupied and empty states is inverted or “twisted” for surface or edge states basically due to a strong spin-orbit interaction Δ_{so} (namely, $\Delta_{\text{so}} = 4.2$ meV for silicene). Although ordinary band insulators can also support conducting metallic states on the surface, topological surface states have special features due to symmetry protection, which make them immune to scattering from ordinary defects and can carry electrical currents even in the presence of large energy barriers.

The low energy electronic properties of a large family of topological insulators and superconductors are well described by the Dirac equation [1], in particular, some 2D gapped Dirac materials isostructural with graphene like: silicene, germanene, stannene, etc. Compared to graphene, these materials display a large spin-orbit coupling and show quantum spin Hall effects [2, 3]. Applying a perpendicular electric field $\mathcal{E}_z = \Delta_z/l$ (l is the inter-lattice distance of the buckled honeycomb structure, namely $l = 0.22\text{\AA}$ for silicene) to the material sheet, generates a tunable band gap (Dirac mass) $\Delta_s^\xi = (\Delta_z - s\xi\Delta_{\text{so}})/2$ ($s = \pm 1$ and $\xi = \pm 1$ denote spin and valley, respectively). There is a topological phase transition [4] from a topological insulator (TI, $|\Delta_z| < \Delta_{\text{so}}$) to a band insulator (BI, $|\Delta_z| > \Delta_{\text{so}}$), at a charge neutrality point (CNP) $\Delta_z^{(0)} = s\xi\Delta_{\text{so}}$, where there is a gap cancellation between the perpendicular electric field and the spin-orbit coupling, thus exhibiting the aforementioned semimetal behavior. In general, a TI-BI transition is

characterized by a band inversion with a level crossing at some critical value of a control parameter (electric field, quantum well thickness [3], etc).

Topological phases are characterized by topological charges like Chern numbers. For an insulating state $|\psi(k)\rangle$, a “gauge potential” $a_j(k) = -i\langle\psi(k)|\partial_{k_j}\psi(k)\rangle$ can be defined in momentum space (k_x, k_y) , so that the Chern number C is the integral $C = \int d^2k f(k)/2\pi$ of the Berry curvature $f = \partial_{k_x}a_y - \partial_{k_y}a_x$ over the first Brillouin zone. When the Hamiltonian is given by (1), the Chern number is obtained as $C_s^\xi = -\xi \text{sgn}(\Delta_s^\xi)/2$, so that a topological insulator phase transition (TIPT) occurs when the sign of the Dirac mass Δ_s^ξ changes [5].

In this article we propose the use of the inverse participation ratio (IPR) of Hamiltonian eigenvectors as a characterization of the topological phases TI and BI. The IPR measures the spread of a state $|\psi\rangle$ over a basis $\{|i\rangle\}_{i=1}^N$. More precisely, if p_i is the probability of finding the (normalized) state $|\psi\rangle$ in $|i\rangle$, then the IPR is defined as $I_\psi = \sum_i p_i^2$. If $|\psi\rangle$ only “participates” of a single state $|i_0\rangle$, then $p_{i_0} = 1$ and $I_\psi = 1$ (large IPR), whereas if $|\psi\rangle$ equally participates on all of them (equally distributed), $p_i = 1/N, \forall i$, then $I_\psi = 1/N$ (small IPR). Therefore, the IPR is a measure of the localization of $|\psi\rangle$ in the corresponding basis. Equivalently, the (Rényi) entropy $S_\psi = -\ln I_\psi$ is a measure of the delocalization of $|\psi\rangle$. We shall see that electron and hole IPR curves cross at the CNP, as a function of the electric field Δ_z , and the crossing IPR value turns out to be an universal quantity, independent of Hamiltonian parameters. Moreover, the different monotonic character (slopes’ sign) of combined (electron plus holes) IPRs in the TI and BI regions turn out to characterize both phases.

These and related information theoretic and statistical measures have proved to be useful in the description and characterization of quantum phase transitions (QPTs) of several paradigmatic models like: Dicke model of atom-field interactions [6–10], vibron model of molecules [11–13] and the ubiquitous Lipkin-Meshkov-Glick model [14, 15]. An important difference between QPT and TIPT is that the first case entails an abrupt symmetry change and the second one does not (necessarily). However, the use of information theoretic measures, like Wehrl entropy [16] and uncertainty relations [17], has proved to be useful to characterize TIPTs too. Moreover, we must also say that strong fluctuations of eigenfunctions (characterized by a set IPRs) also represent one of the hallmarks of the traditional Anderson metal-insulator transition [18–22]. In fact, the phenomenon of localization of the electronic wave function can be regarded as the key manifestation of quantum coherence at a macroscopic scale in a condensed matter system.

The paper is organized as follows. Firstly, in Section II, we shall introduce the low energy Hamiltonian describing the electronic properties of some 2D Dirac materials like silicene, germanene, stantene, etc, in the presence of perpendicular electric and magnetic fields. Then, in Section III, we will compute the IPR of Hamiltonian eigenvectors and we shall discuss the (different) structure of IPR curves as a function of the electric field across TI and BI regions. Section IV is devoted to final comments and conclusions.

II. LOW ENERGY HAMILTONIAN

The low energy dynamics of a large family of topological insulators (namely, honeycomb structures) is described by the Dirac Hamiltonian in the vicinity of the Dirac points $\xi = \pm 1$ [23]

$$H_s^\xi = v(\xi\sigma_x p_x + \sigma_y p_y) - \frac{1}{2}\xi s\Delta_{\text{so}}\sigma_z + \frac{1}{2}\Delta_z\sigma_z, \quad (1)$$

where σ_j are the usual Pauli matrices, v is the Fermi velocity of the corresponding material (namely, $v = 4.2 \times 10^5 \text{ m/s}$ for silicene) and Δ_{so} and Δ_z are the spin-orbit and electric field couplings. The application of a perpendicular magnetic field B is implemented through the minimal coupling $\vec{p} \rightarrow \vec{p} + e\vec{A}$ for the momentum, where $\vec{A} = (-By, 0)$ is the vector potential in the Landau gauge. The Hamiltonian eigenvalues and eigenvectors at the ξ points are given by [23]

$$E_n^{s\xi} = \begin{cases} \text{sgn}(n)\sqrt{|n|\hbar^2\omega^2 + (\Delta_s^\xi)^2}, & n \neq 0, \\ -\xi\Delta_s^\xi, & n = 0, \end{cases} \quad (2)$$

and

$$|n\rangle_s^\xi = \begin{pmatrix} -iA_n^{s\xi}||n| - \xi_+\rangle \\ B_n^{s\xi}||n| - \xi_-\rangle \end{pmatrix}, \quad (3)$$

where we denote by $\xi_\pm = (1 \pm \xi)/2$, the Landau level index $n = 0, \pm 1, \pm 2, \dots$, the cyclotron frequency $\omega = v\sqrt{2eB/\hbar}$, the lowest band gap $\Delta_s^\xi \equiv (\Delta_z - s\xi\Delta_{\text{so}})/2$ and the coefficients $A_n^{s\xi}$ and $B_n^{s\xi}$ are given by [23]

$$\begin{aligned} A_n^{s\xi} &= \begin{cases} \text{sgn}(n)\sqrt{\frac{|E_n^{s\xi}| + \text{sgn}(n)\Delta_s^\xi}{2|E_n^{s\xi}|}}, & n \neq 0, \\ \xi_-, & n = 0, \end{cases} \\ B_n^{s\xi} &= \begin{cases} \sqrt{\frac{|E_n^{s\xi}| - \text{sgn}(n)\Delta_s^\xi}{2|E_n^{s\xi}|}}, & n \neq 0, \\ \xi_+, & n = 0, \end{cases} \end{aligned} \quad (4)$$

The vector $||n\rangle$ denotes an orthonormal Fock state of the harmonic oscillator. We are discarding a trivial plane-wave dependence e^{ikx} in the x direction that does not affect our IPR calculations, which only depend on the y direction in this gauge.

As already stated, there is a prediction (see e.g. [24–27]) that when the gap $|\Delta_s^\xi|$ vanishes at the CNP $|\Delta_z| = \Delta_{\text{so}}$, silicene undergoes a phase transition from a topological insulator (TI, $|\Delta_z| < \Delta_{\text{so}}$) to a band insulator (BI, $|\Delta_z| > \Delta_{\text{so}}$). This topological phase transition entails an energy band inversion. Indeed, in Figure 1 we show the low energy spectra (2) as a function of the external electric potential Δ_z for $B = 0.01 \text{ T}$. One can see that there is a band inversion for the $n = 0$ Landau level (either for spin up and down) at both valleys. The energies $E_0^{1,\xi}$ and $E_0^{-1,\xi}$ have the same sign in the BI phase and different sign in the TI phase, thus distinguishing both regimes. We will provide an alternative description of this phenomenon in terms of IPR relations for the Hamiltonian eigenstates (3), thus providing a quantum-information characterization of TIPT.

III. IPR AND TOPOLOGICAL INSULATOR PHASE TRANSITION

The IPR of a given state I_ψ is related to a certain basis. In this article we shall chose the position representation to write the Hamiltonian eigenstates (3). We know that Fock (number) states $|n\rangle$ can be written in position representation as

$$\langle y|n\rangle = \frac{\omega^{1/4}}{\sqrt{2^n n! \sqrt{\pi}}} e^{-\omega y^2/2} H_n(\sqrt{\omega}y) \quad (5)$$

where H_n are the Hermite polynomials of degree n . The number-state density in position space is $\rho_n(y) = |\langle y|n\rangle|^2$, which is normalized according to $\int \rho_n(y) dy = 1$. Now, taking into account Eq. (3), the density for the Hamiltonian eigenvectors (3) in position representation is given by

$$\rho_n^{s\xi}(y) = (A_n^{s\xi})^2 |\langle y|n| - \xi_+\rangle_s^\xi|^2 + (B_n^{s\xi})^2 |\langle y|n| - \xi_-\rangle_s^\xi|^2. \quad (6)$$

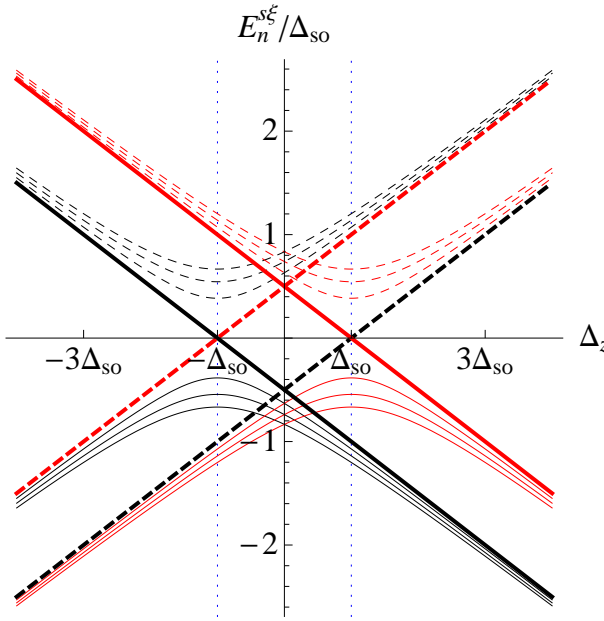


FIG. 1: Low energy spectra of silicene as a function of the external electric potential Δ_z for $B = 0.01$ T. Landau levels $n = \pm 1, \pm 2$ and ± 3 , at valley $\xi = 1$, are represented by dashed (electrons) and solid (holes) thin lines, black for $s = -1$ and red for $s = 1$ (for the other valley we simply have $E_n^{s,-\xi} = E_n^{-s,\xi}$). The lowest Landau level $n = 0$ is represented by thick lines at both valleys: solid at $\xi = 1$ and dashed at $\xi = -1$. Vertical blue dotted grid lines indicate the CNPs separating BI ($|\Delta_z| > \Delta_{\text{so}}$) from TI ($|\Delta_z| < \Delta_{\text{so}}$) phases.

The IPR of a Hamiltonian eigenstate in position representation is then calculated as

$$I_n^{s\xi} \equiv \int_{-\infty}^{\infty} (\rho_n^{s\xi}(y))^2 dy. \quad (7)$$

As a previous step, we need the following integrals of Hermite density products:

$$\begin{aligned} M_{n,m} &\equiv \int_{-\infty}^{\infty} \rho_n(y) \rho_m(y) dy = \\ &= \sqrt{\frac{\omega}{2\pi}} \begin{pmatrix} 1 & \frac{1}{2} & \frac{3}{8} & \frac{5}{16} & \dots \\ \frac{1}{2} & \frac{3}{4} & \frac{41}{16} & \frac{115}{32} & \dots \\ \frac{3}{8} & \frac{4}{7} & \frac{41}{32} & \frac{31}{128} & \dots \\ \frac{5}{16} & \frac{11}{32} & \frac{64}{128} & \frac{147}{256} & \dots \\ \vdots & \vdots & \vdots & \vdots & \ddots \end{pmatrix}, \end{aligned} \quad (8)$$

for $n, m = 0, 1, 2, 3, \dots$. We shall also restrict ourselves to the valley $\xi = 1$, omitting this index from (3) and (4). All the results for the valley $\xi = 1$ are straightforwardly translated to the valley $\xi = -1$ by swapping electrons for holes (i.e., $n \leftrightarrow -n$) and spin up for down (i.e., $s \leftrightarrow -s$). Taking into account all these considerations, the IPR of a Hamiltonian eigenstate is explicitly written as

$$\begin{aligned} I_n^s &\equiv (A_n^s)^4 M_{|n|-1,|n|-1} + (B_n^s)^4 M_{|n|,|n|} \\ &+ 2(A_n^s B_n^s)^2 M_{|n|,|n|-1}. \end{aligned} \quad (9)$$

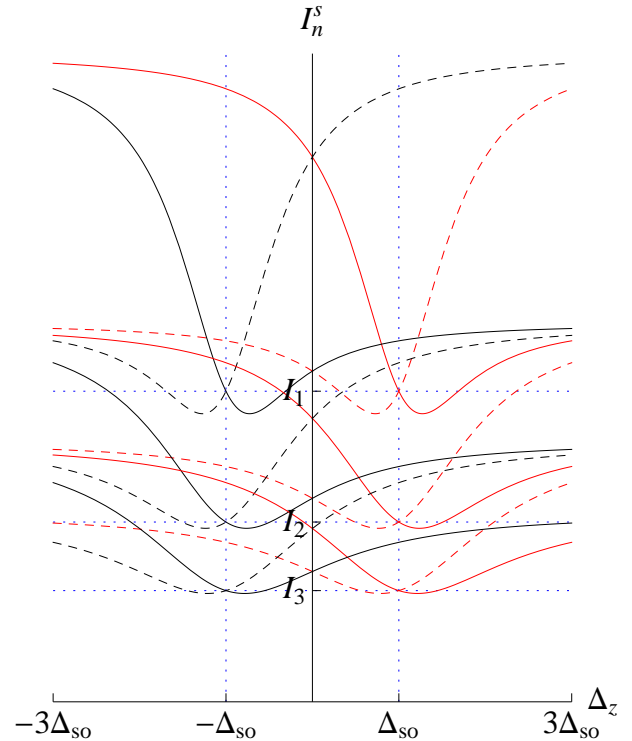


FIG. 2: IPR $I_n^{s\xi}$ in position space at valley $\xi = 1$ as a function of the electric potential Δ_z for the Landau levels: $n = \pm 1, \pm 2$ and ± 3 and magnetic field $B = 0.01$ T. Electron IPR curves are dashed and hole curves are solid, black for spin down $s = -1$ and red for spin up $s = 1$. Electron and hole IPR curves cross at the critical value of the electric potential $\Delta_z^{(0)} = s\Delta_{\text{so}}$; vertical blue dotted grid lines indicate this CNPs and horizontal blue dotted grid lines indicate the crossing IPR values (10).

In Figure 2 we plot I_n^s as a function of the external electric potential Δ_z for the Landau levels: $n = \pm 1, \pm 2$ and ± 3 . Electron and hole IPR curves cross at the CNPs $\Delta_z^{(0)} = s\Delta_{\text{so}}$, where they take the values:

$$I_1 = \sqrt{\frac{\omega}{2\pi}} \frac{11}{16}, \quad I_2 = \sqrt{\frac{\omega}{2\pi}} \frac{145}{256}, \quad I_3 = \sqrt{\frac{\omega}{2\pi}} \frac{515}{1024}. \quad (10)$$

Note that, except for ω , the critical crossing IPR value I_n only depends on the Landau level n , and not on any other physical magnitude, thus providing a universal characterization of the topological insulator transition. We have checked that the smaller the magnetic field strength, the greater the slope of the electron-hole IPR curves at the CNP. The asymptotic values $I_n(\pm\infty) = \lim_{\Delta_z \rightarrow \pm\infty} I_n^s(\Delta_z)$ also exclusively depend on $n = 1, 2, \dots$ and ω , and are:

$$I_1(\infty) = \sqrt{\frac{\omega}{2\pi}} \frac{1}{16}, \quad I_2(\infty) = \sqrt{\frac{\omega}{2\pi}} \frac{3}{4}, \quad I_3(\infty) = \sqrt{\frac{\omega}{2\pi}} \frac{41}{64}, \dots \quad (11)$$

fulfilling $I_{-n}(-\infty) = I_n(\infty)$ and $I_{-n}(\infty) = I_{|n|+1}(\infty)$.

The crossing of IPR curves for electron and holes characterizes the CNPs. However, in order to properly char-

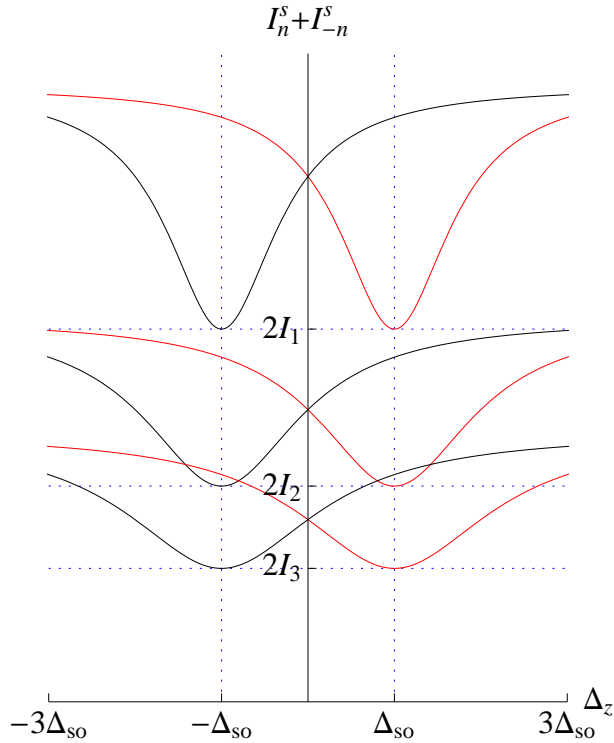


FIG. 3: Combined IPR $I_n^{s\xi} + I_{-n}^{s\xi}$ of electron plus holes at valley $\xi = 1$ as a function of the electric potential Δ_z for the Landau levels: $n = \pm 1, \pm 2$ and ± 3 and magnetic field $B = 0.01\text{T}$. Black curves for $s = -1$ and red for $s = 1$. Vertical blue dotted grid lines indicate the CNPs and horizontal blue dotted grid lines indicate the minimum combined IPR values.

acterize TI and BI phases, the combined IPR of electrons plus holes, $Y_n^s = I_n^s + I_{-n}^s$, offers a better indicator of the corresponding transition (see Figure 3). Indeed, on the one hand, Y_n^s display global minima at the CNPs (highly delocalized states); on the other hand, the quantity

$$C(\Delta_z) = \text{sgn} \left(\frac{\partial Y_s}{\partial \Delta_z} \frac{\partial Y_{-s}}{\partial \Delta_z} \right), \quad (12)$$

plays the role of a “topological charge” (like a Chern number) so that

$$C(\Delta_z) = \begin{cases} 1, & |\Delta_z| > \Delta_{\text{so}} \text{ BI}, \\ -1, & |\Delta_z| < \Delta_{\text{so}} \text{ TI}. \end{cases} \quad (13)$$

That is, the sign of the product of combined IPR slopes for spin up and down, clearly characterizes the two (TI and BI) phases.

The product $I_n^s \times I_{-n}^s$ of electron times hole IPRs also exhibits a critical behavior at the CNPs and characterizes both phases. Actually, the combined entropy ($S = -\ln I$)

$$S_n^s + S_{-n}^s = -\ln(I_n^s \times I_{-n}^s), \quad (14)$$

is minimum at the CNPs (highly delocalized states), as can be appreciated in Figure 4. For the quotient $Q_n^s \equiv$

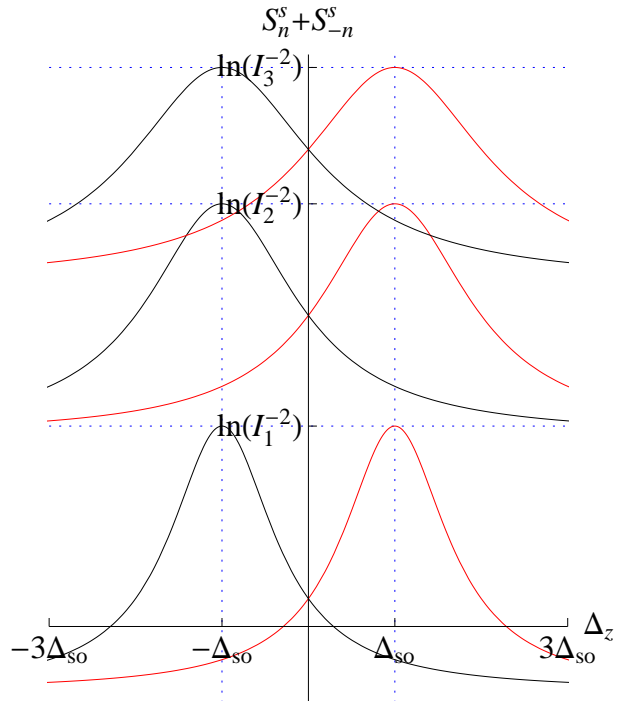


FIG. 4: Combined entropies $S_n^{s\xi} + S_{-n}^{s\xi}$ ($S = -\ln I$) of electron plus holes at valley $\xi = 1$ as a function of the electric potential Δ_z for the Landau levels: $n = \pm 1, \pm 2$ and ± 3 and magnetic field $B = 0.01\text{T}$. Same color code as in Fig. 3. Minimum entropies are attained at the CNPs and are indicated by horizontal blue gris lines.

I_n^s / I_{-n}^s we have that the quantity

$$\text{sgn} \left(\frac{Q_n^s(\Delta_z) - 1}{Q_n^{-s}(\Delta_z) - 1} \right) = \begin{cases} 1, & |\Delta_z| > \Delta_{\text{so}} \text{ BI}, \\ -1, & |\Delta_z| < \Delta_{\text{so}} \text{ TI}, \end{cases} \quad (15)$$

also characterizes both phases, as can be explicitly appreciated in Figure 5.

IV. CONCLUSIONS

We have studied localization properties of the Hamiltonian eigenvectors $|n\rangle_s^\xi$ (n, ξ, s denote: Landau level, valley and spin, respectively) for 2D Dirac materials isostructural with graphene (namely, silicene) in the presence of perpendicular magnetic B and electric Δ_z fields. The electric field provides a tunable band gap $\Delta_s^\xi = (\Delta_z - s\xi\Delta_{\text{so}})/2$ which is “twisted” at the charge neutrality points (CNPs) $|\Delta_z| = \Delta_{\text{so}}$, for surface states, due to a strong spin-orbit interaction Δ_{so} . The topological insulator (TI) and band insulator (BI) phases are then characterized by $|\Delta_z| < \Delta_{\text{so}}$ and $|\Delta_z| > \Delta_{\text{so}}$, respectively, or by the sign of Δ_s^ξ (the Chern number).

We have proposed information-theoretic measures, based on the inverse participation ratio $I_n^{s\xi}$ (IPR), as alternative signatures of a topological insulator phase transition. The IPR measures the localization of a state in

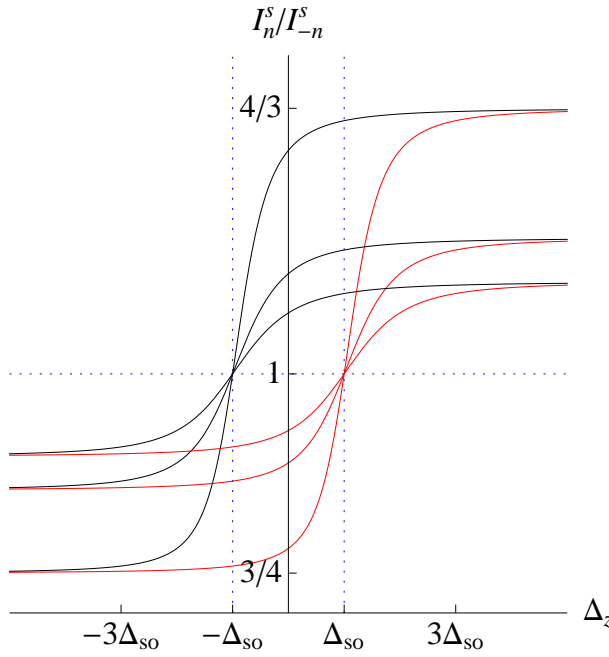


FIG. 5: Electron-hole IPR quotients I_n^s / I_{-n}^s at valley $\xi = 1$ as a function of the electric potential Δ_z for the Landau levels: $n = \pm 1, \pm 2$ and ± 3 and magnetic field $B = 0.01\text{T}$. Same color code as in Fig. 3. Electron-hole IPR ratios are increasing functions of Δ_z .

the corresponding basis (position representation in our case). We have seen that IPR curves $I_n^s(\Delta_z)$ of electrons ($n > 0$) and holes ($n < 0$) cross at the CNPs, the crossing value being a universal quantity basically depending on the Landau level n . The combined IPR $Y_n^s = I_n^s + I_{-n}^s$ of electrons plus holes is minimum at the CNPs; i.e. the combined state is highly delocalized (maximum entropy) at the transition point. The different monotonic behavior of combined Y_n^s and quotient $Q_n^s \equiv I_n^s / I_{-n}^s$ IPR curves across BI and TI regions provides topological (Chern-like) numbers (12) and (15) which characterize both phases.

Therefore, as it already happens for the traditional Anderson metal-insulator transition, we have shown that fluctuations of Hamiltonian eigenfunctions (characterized by IPRs) also describe topological-band insulator transitions.

Acknowledgments

The work was supported by the Spanish projects: MINECO FIS2014-59386-P, CEIBIOTIC-UGR PV8 and the Junta de Andalucía projects FQM.1861 and FQM-381.

[1] Shun-Qing Shen, *Topological Insulators: Dirac Equation in Condensed Matters*, Springer-Verlag Berlin Heidelberg 2012.

[2] Kane C L and Mele E J, Phys. Rev. Lett. **95**, 226801 (2005)

[3] B. Andrei Bernevig, Taylor L. Hughes and Shou-Cheng Zhang, Science **314**, 1757-1761 (2006).

[4] M. Tahir, U. Schwingenschlögl, Scientific Reports, **3**, 1075 (2013).

[5] M. Ezawa, Monolayer Topological Insulators: Silicene, Germanene and Stanene, arXiv:1503.08914

[6] E. Romera, and Á. Nagy, Phys. Lett. A **375**, 3066 (2011).

[7] E. Romera, K. Sen, Á. Nagy, J. Stat. Mech. P09016 (2011).

[8] E. Romera, M. Calixto and Á. Nagy, EPL, **97**, 20011 (2012).

[9] M. Calixto, Á. Nagy, I. Paradela and E. Romera, Phys. Rev. A **85**, 053813 (2012)

[10] E. Romera, R. del Real, M. Calixto, Phys. Rev. A **85**, 053831, (2012).

[11] M. Calixto, R. del Real, E. Romera, Phys. Rev. A **86**, 032508 (2012).

[12] M. Calixto, E. Romera, and R. del Real, J. Phys. A **45**, 365301 (2012).

[13] M. Calixto and F. Pérez-Bernal, Phys. Rev. A **89**, 032126 (2014).

[14] E. Romera, M. Calixto and O. Castaños, Physica Scripta **89**, 095103 (2014)

[15] M. Calixto, O. Castaños and E. Romera, EPL **108**, 47001 (2014).

[16] M. Calixto and E. Romera, EPL **109**, 40003 (2015)

[17] E. Romera and M. Calixto, J. Phys.: Condens. Matter **27**, 175003 (2015)

[18] P.W. Anderson, Phys. Rev. **109**, 1492 (1958).

[19] F. Wegner, Z. Phys. B **36**, 209 (1980)

[20] T. Brandes, S. Kettemann, *Anderson Localization and Its Ramifications: Disorder, Phase Coherence and Electron Correlations*, Lecture Notes in Physics **630**, Springer 2003

[21] F. Evers and A. D. Mirlin, Rev. Mod. Phys. **80**, 1355 (2008)

[22] C. Aulbach, A. Wobst, G.-L. Ingold, P. Hanggi, and I. Varga, New J. Phys. **6**, 70 (2004).

[23] C.J. Tabert and E.J. Nicol, Phys. Rev. Lett. **110**, 197402 (2013); C.J. Tabert and E.J. Nicol, Phys. Rev. B **88**, 085434 (2013).

[24] N. D. Drummond, V. Zólyomi, and V. I. Fal'ko, Phys. Rev. B **85**, 075423 (2012).

[25] C. C. Liu, W. Feng, and Y. Yao, Phys. Rev. Lett. **107**, 076802 (2011).

[26] C. C. Liu, H. Jiang, and Y. Yao, Phys. Rev. B **84**, 195430 (2011).

[27] M. Ezawa, New Journal of Physics **14** (2012) 033003